Cell Reports, Volume *42*

Supplemental information

Epinephrine inhibits PI3Kα via the Hippo kinases

Ting-Yu Lin, Shakti Ramsamooj, Tiffany Perrier, Katarina Liberatore, Louise Lantier, Neil Vasan, Kannan Karukurichi, Seo-Kyoung Hwang, Edward A. Kesicki, Edward R. Kastenhuber, Thorsten Wiederhold, Tomer M. Yaron, Emily M. Huntsman, Mengmeng Zhu, Yilun Ma, Marcia N. Paddock, Guoan Zhang, Benjamin D. Hopkins, Owen McGuinness, Robert E. Schwartz, Baran A. Ersoy, Lewis C. Cantley, Jared L. Johnson, and Marcus D. Goncalves

Supplemental Information

Epinephrine inhibits PI3K alpha via the Hippo kinases.

Ting-Yu Lin, Shakti Ramsamooj, Tiffany Perrier, Katarina Liberatore, Louise Lantier, Neil Vasan, Kannan Karukurichi, Seo-Kyoung Hwang, Edward A. Kesicki, Edward R. Kastenhuber, Thorsten Wiederhold, Tomer M. Yaron, Emily M. Huntsman, Mengmeng Zhu, Yilun Ma, Marcia N. Paddock, Guoan Zhang, Benjamin D. Hopkins, Owen McGuinness, Robert E. Schwartz, Baran A. Ersoy, Lewis C. Cantley, Jared L. Johnson, and Marcus D. Goncalves

Supplemental Table 1 Data collection, reduction and refinement statistics

	T1061Ep110/p85/GDC0077
Data reduction	
Space group	$P2_12_12_1$
Cell dimensions	
a, *b*, *c* (Å)	99.81, 107.68, 136.30
α, β, γ (°)	90, 90, 90
Resolution range (Å)	47.39-2.44 (2.63-2.44)
Total number of reflections	834794 (42812)
Number of unique reflections	44827 (2241)
Ellipsoidal completeness (%)	94.9 (56.7)
Spherical completeness (%)	80.7 (20.3)
Redundancy	18.6 (19.1)
$I / \sigma I$	8.2 (1.4)
$CC_{1/2}$	0.996 (0.648)
R_{meas}	0.28 (2.40)
R_{merge}	0.28 (2.33)
Refinement	
Resolution (Å)	2.82
No. reflections	36173 (724)
R_{work}	0.285 (0.363)
R_{free}	0.300 (0.332)
No. atoms	10845
Protein	10604
Ligand/ion	52
Water	189
B-factors	68.7
Protein	69.2
Ligand/ion	55.6
Water	44.0
R.m.s. deviations	
Bond lengths (Å)	0.007
Bond angles (°)	0.750

*Values in parentheses are for highest-resolution shell.

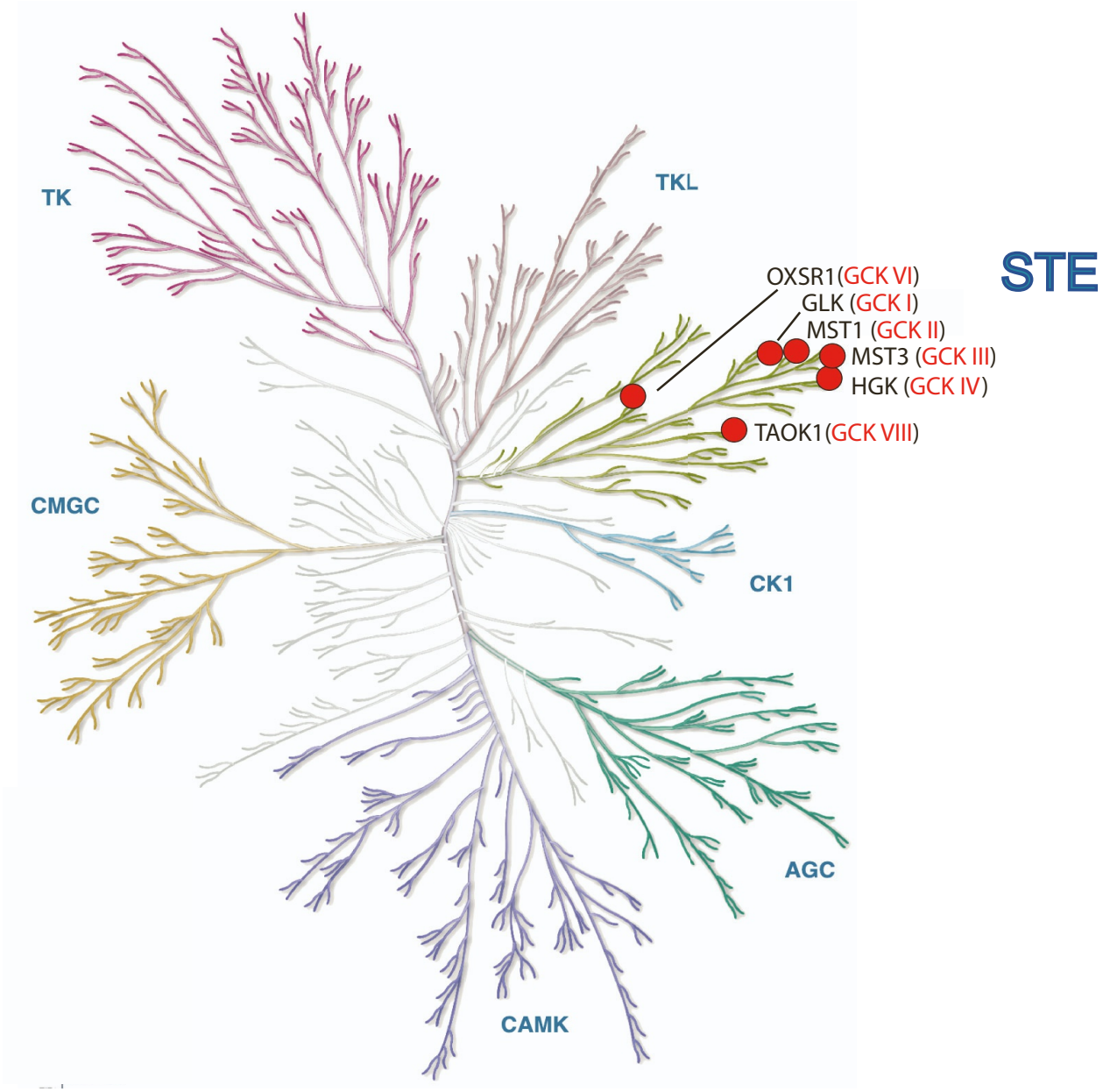

Figure S1. The GCK family kinases.

Six GCK family members selected for PI3Kα activity screens. Their positions are highlighted on the evolutionary dendrogram of the human protein kinome.

A.

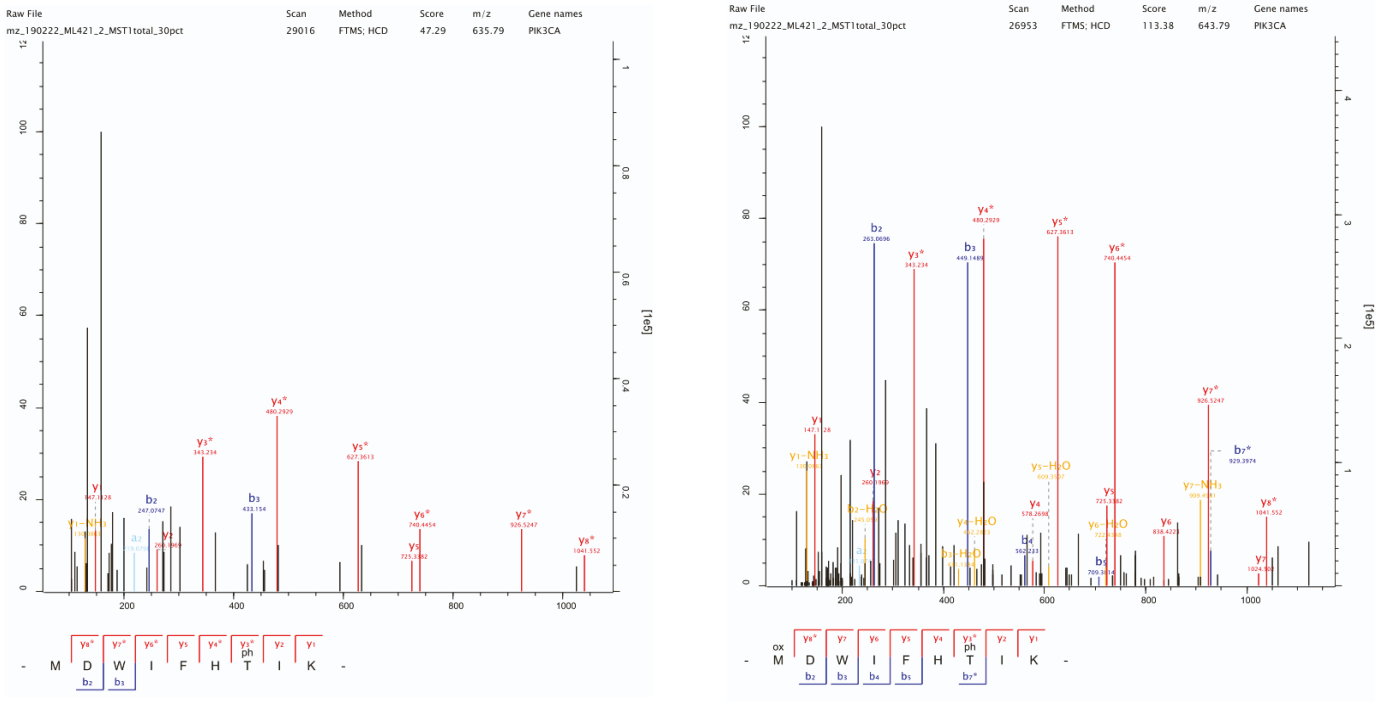

B.

Figure S2. MST1/2 and HGK inhibit catalytic activity of p110α through phosphorylation at T1061.

(A) Phosphopeptides containing T1061 were identified by MS/MS using purified p110α/p85α incubated with MST1 for 1h. Two versions of phosphopeptides were identified, with differences in methionine oxidation status. (B) Autoradiography of [^{32}P]PIP$_3$ production by the purified p110α (WT)/p85α or p110α (T1061A)/p85α after treatment with MST1 or HGK.

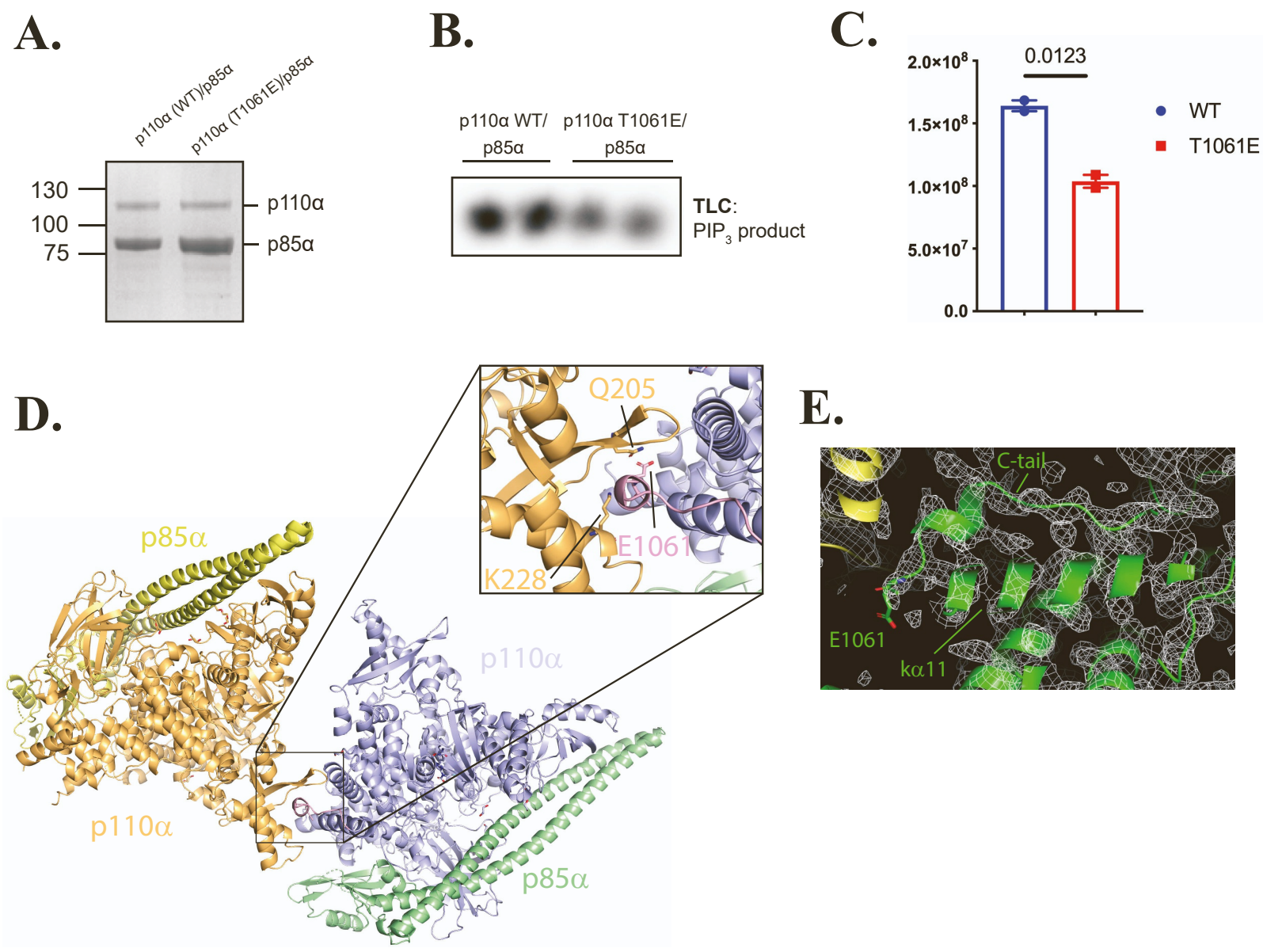

Figure S3. Characterization of the phosphomimetic T1061 p110a mutant.

(A) Top: Coomassie stain comparison of purified recombinant p110a (WT)/His_6-p85a and p110a (T1061E)/His_6-p85a. (B) Basal activities of p110α (WT) and the phosphomimetic mutant, p110α (T1061E) as measured by [^{32}P]-PIP_3 production using thin layer chromatography. Experiments were normalized to amounts of p110a. (C) Quantification of densitometry from (B). Data is represented as means ± SEMs. Significance was calculated using student's t test (N=2). (D) Structural model of p110a (T1061E)/p85a-niSH2, illustrating crystal contacts between E1061 and residues on a separate heterodimer. (E) Structural model and electron density map (mesh level 1.0) of C-terminus and helix ka11 of p110a (T1061E)/p85a-niSH2.

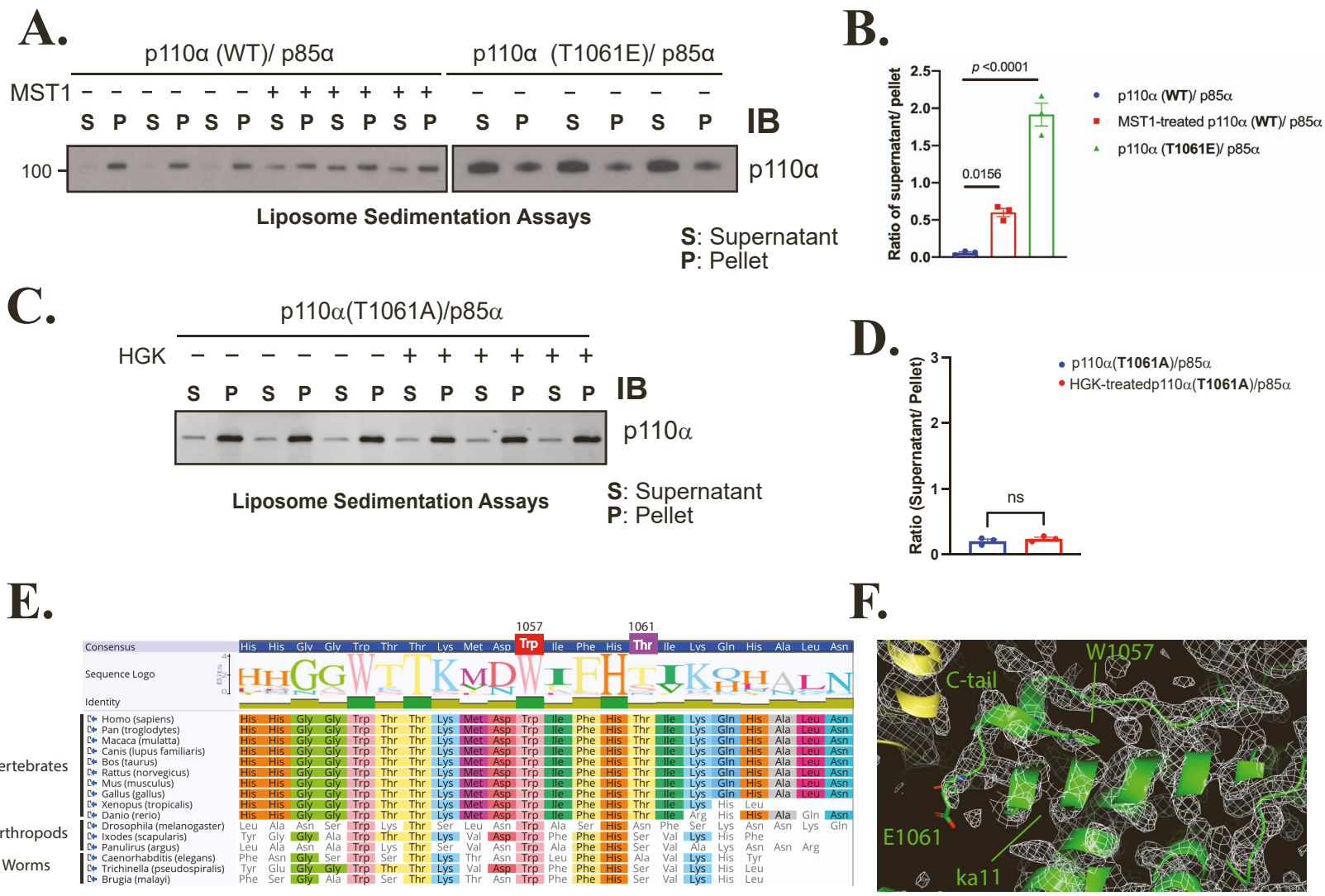

Figure S4. Phosphorylation of p110α by the Hippo kinases impedes p110α's interaction with membranes.

(A) Liposome sedimentation assays of PI3Kα -/+ MST1 and untreated phosphomimetic mutant p110α (T1061E)/p85α. Immunoblots of p110α recovered from pellet (P) and supernatant (S). N=3 (B) Quantification of corresponding densitometries from (A): as ratios of p110α recovery from supernatant over pellet. (C) Liposome sedimentation assays of PI3Kα (T1061A)/p85α -/+ HGK. (D) Quantification of corresponding densitometries from (C): as ratios of p110α recovery from supernatant over pellet. (E) Evolutionary alignment of the C-tails of p110α orthologs, highlighting W1057 and T1061. (F) Structural model and electron density map from (S3E) illustrating the position of the sidechain of W1057. Bar graphs represent Mean ± SEMs. Significance was calculated using one-way ANOVA with Turkey's multiple comparisons post-test (panel B), and student's t-test (panel D).

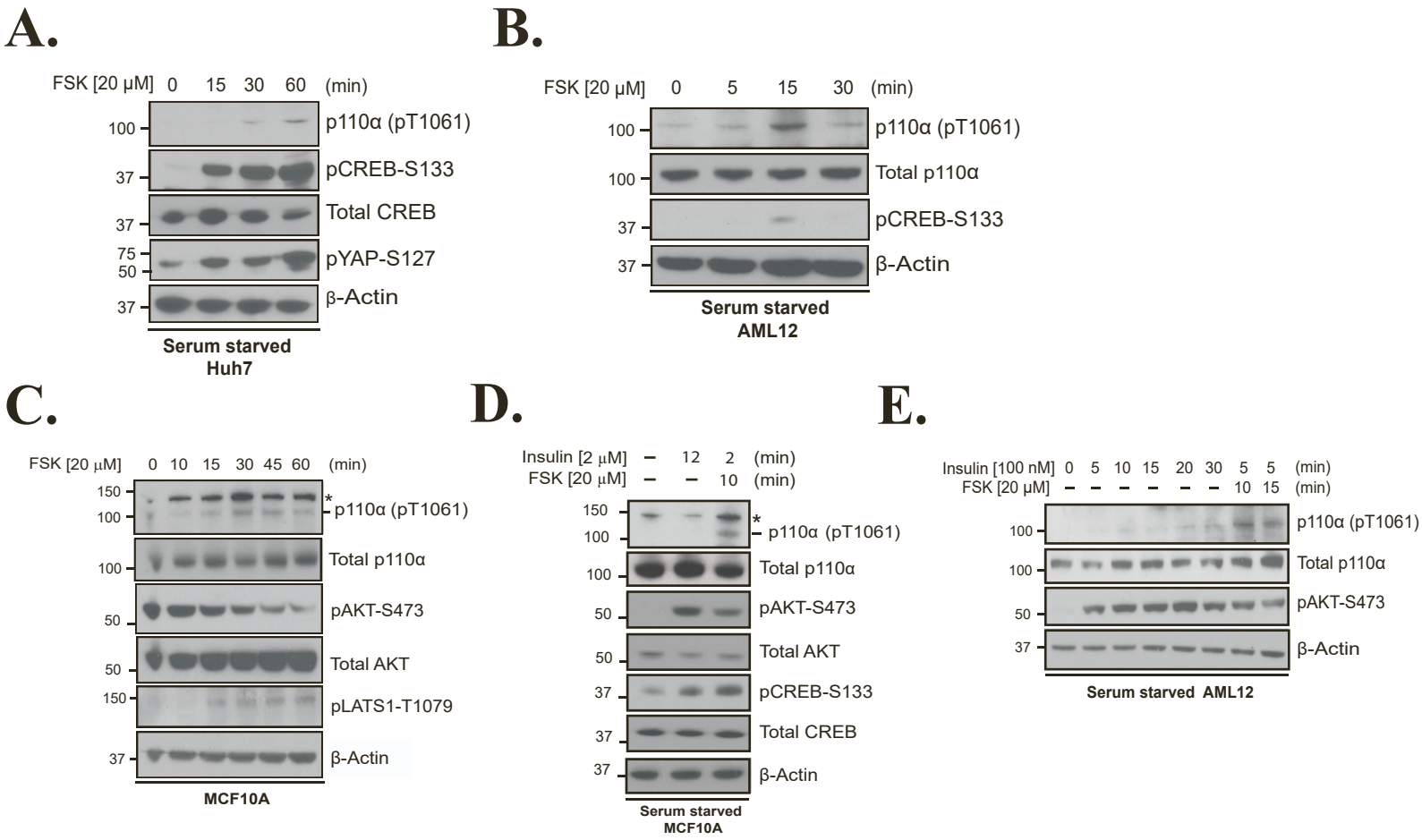

Figure S5. Activation of adenylyl cyclase promotes phosphorylation and inhibition of p110α.

(A) Immunoblot for the indicated proteins using lysates from Huh7 cells that were serum starved for 12 h before stimulated with FSK [20 μM] for 0, 15, 30 and 60 min. (B) Immunoblot for the indicated proteins using lysates from AML12 cells that were serum starved for 12 h before stimulated with FSK [20 μM] for 0, 5, 15 and 30 min. (C) Immunoblot for the indicated proteins using lysates from MCF10A cells cultured in full medium that were stimulated with FSK [20 μM] for 0, 10, 15, 30, 45, and 60 min. (D) Immunoblot for the indicated proteins using lysates from MCF10A cells that were serum starved for 16 h, and then stimulated with DMSO, insulin [2 μM], or insulin [2 μM] followed by FSK [20 μM] for 10 min. *: non-specific band. (E) Immunoblot for the indicated proteins using lysates from AML12 cells that were serum starved for 12 h before stimulated with insulin [100 nM] for 0, 5, 10, 15, 20 and 30 min or insulin [100 nM] followed by FSK [20 μM] for 10 or 15 min.

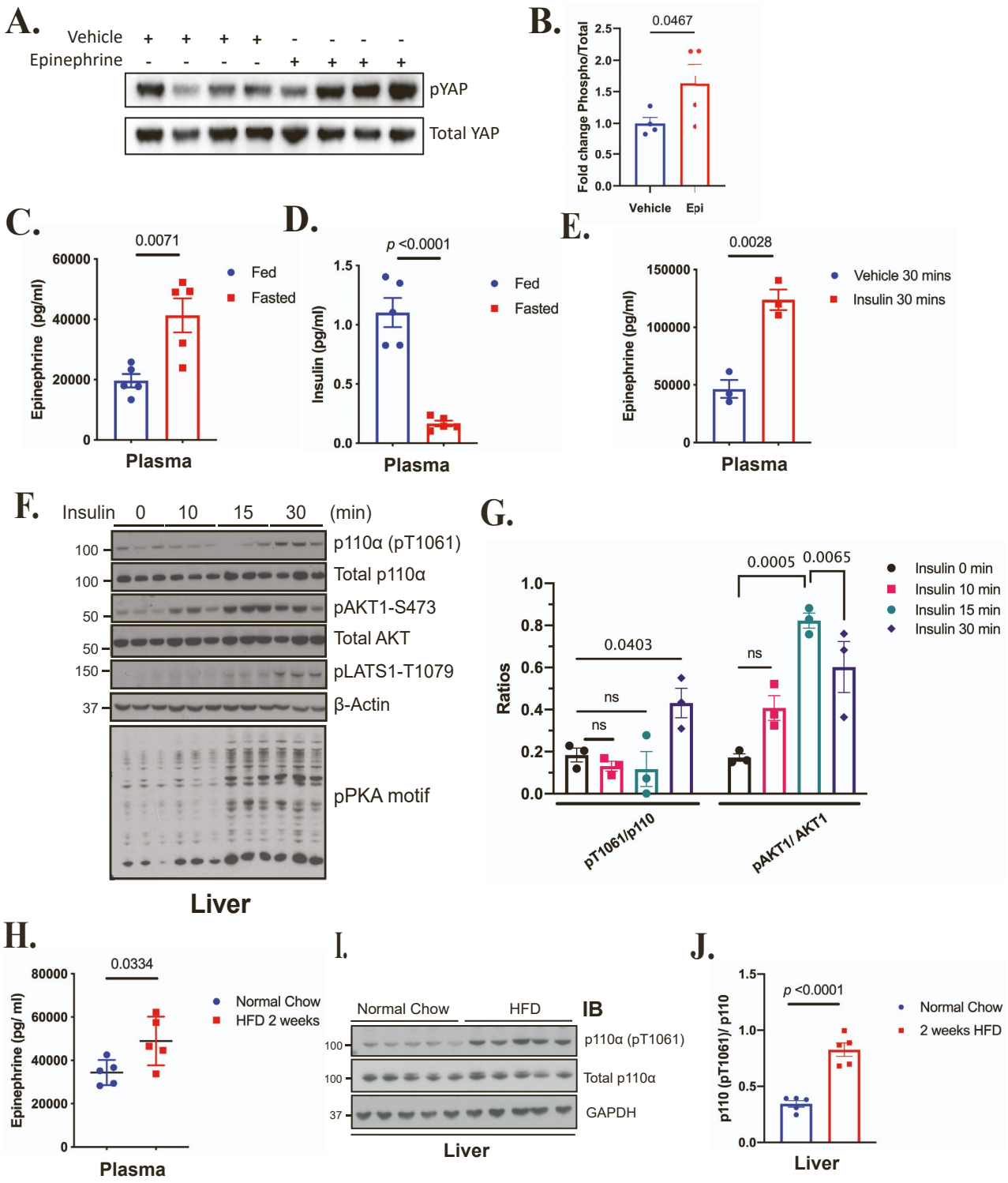

Figure S6. Epinephrine promotes phosphorylation of p110α and activation of Hippo signaling in vivo.

(A) Immunoblot for the indicated proteins using lysates from livers taken from WT mice injected with vehicle (normal saline) or epinephrine [0.3 µg/g] for 10 min (n=4). (B) Quantification of the ratios of phosphorylated YAP to total YAP using band intensity from A. (C) Plasma epinephrine and (D) insulin levels from WT mice that were fasted for 18 h (Fasted) and then euthanized or provided food for 4 h (Fed). N=5. (E) Plasma epinephrine levels from WT mice that were injected with insulin [0.75 mIU/g] for 0 and 30 min. N=3. (F) Immunoblot for the indicated proteins using lysates from livers taken from WT mice injected with insulin [0.75 mIU/g] for different time periods (0, 10, 15 and 30 min). (G) Quantification of the ratios of phosphorylated p110α (pT1061) to total p110α and pAKT1 to total AKT1 using band intensity from F. (H) Plasma epinephrine levels from WT mice fed either normal chow or 60% high-fat diet (HFD) for 2 weeks. N=5. (I) Immunoblot for the indicated proteins using lysates from liver taken from WT mice fed normal chow or HFD for 2 weeks. (J) Quantification of the ratios of pT1061 to total p110α using band intensity from I. N=5. Data is represented as means ± SEMs. For B, C, D, E, H, J significance was calculated using student's t-test. For H, significance was calculated using ANOVA with Dunnett's post-test.

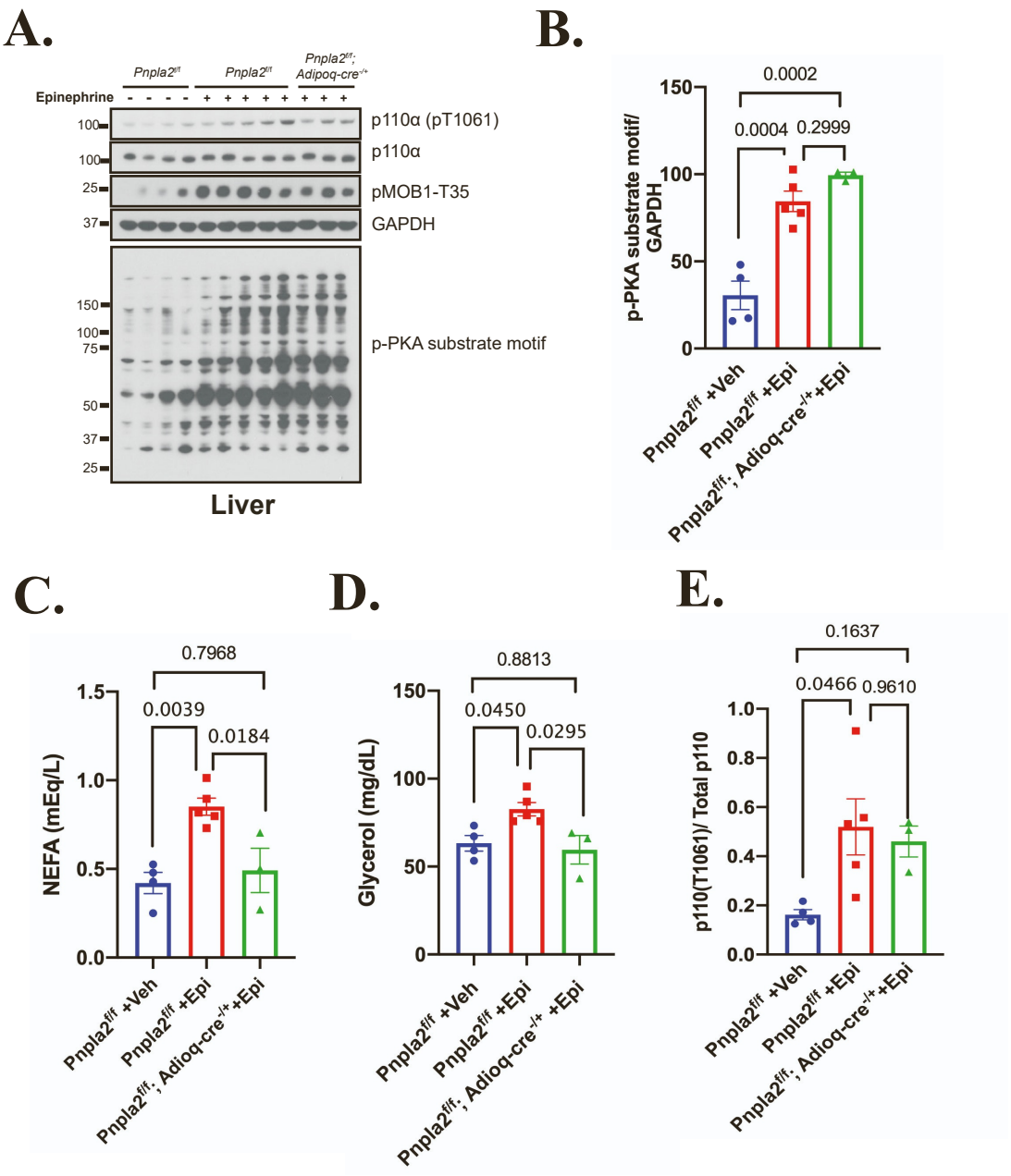

Figure S7. Effects of epinephrine on mice without adipocyte lipolysis.

Lipolysis-deficient mice (Pnpla2$^{f/f}$; Adipoq-Cre$^{+/-}$) and littermate controls (Pnpla2$^{f/f}$) were treated with vehicle (Veh, saline) or epinephrine (Epi) via I.P. injection (N=4, 5, 3). Blood and liver tissue were harvested 10 minutes later. (A) Markers of MST1/2 activation from liver lysates using Western blot. Quantification of combined PKA substrate motif lane normalized to GAPDH. Significance calculated using ANOVA with Turkey's multiple comparisons post-test. Serum (C) non-esterified fatty acids (NEFA) and (D) glycerol from mice in A. Significance calculated using ANOVA with Turkey's multiple comparisons post-test. (E) T1061 p110a phosphorylation normalized to total p110a. Significance calculated using ANOVA with Sidak's multiple comparisons post-test. All data represented as means ± SEMs.

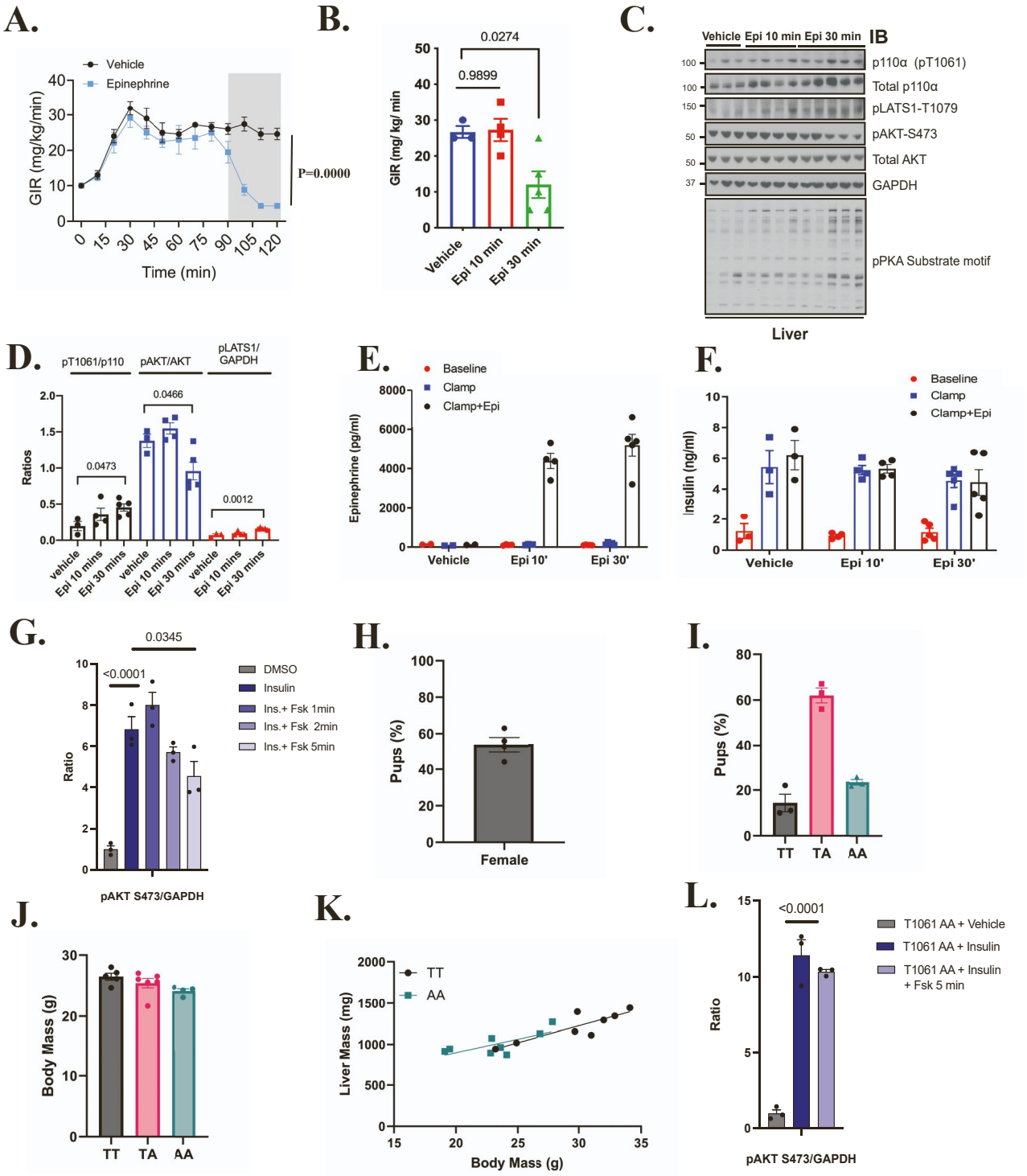

Figure S8 Epinephrine-mediated insulin resistance correlates with T1061 phosphorylation.

(A) Glucose infusion rate (GIR) over time during a hyperinsulinemic-euglycemic clamp (HIEC) performed on WT rats. After 87 min, rats received an infusion of vehicle (normal saline, N=5) or Epi (0.75 µg/kg/min, N=6) for 30 min. (B) Steady-state GIR during HIEC on WT rats where rats received vehicle (normal saline, N=3) or Epi (0.75 µg/kg/min) for either 10 min (N=4) or 30 min (N=5) at the 87 min mark, as depicted in A. (C) Immunoblot for the indicated proteins using lysates from liver taken from WT rats in B. (C) Quantification of the ratio of pT1061 to total p110α, phosphorylated AKT to total AKT, and pLATS1 (T1079) to GAPDH using band intensities from C. (E-F) Measurements of epinephrine and insulin during HIEC in B. (G) Quantification of the ratios of pAKT to GAPDH using band intensity from Fig 5E. N=3. (H) Percentage of female pups and (I) specified genotypes resulting from 3 independent breeding cages with heterozygous x heterozygous ($p110^{T1061A/T}$) crossings. (J) Body weight of each T1061 genotype at 8 weeks of age. N=5, 6, 4 for TT, TA, and AA respectively. (J) Liver mass vs Body mass relationship for T1061 TT and mice (N=8 each) with overlying linear regression. (L) Quantification of the ratios of pAKT to GAPDH using band intensity from Fig 5G. N=3. Bars depict means ± SEMs. For A, significance was calculted using student's t-test for points at 120 min. For B and D, significance was calculated using ANOVA with Dunnett's multiple comparisons to vehicle control.

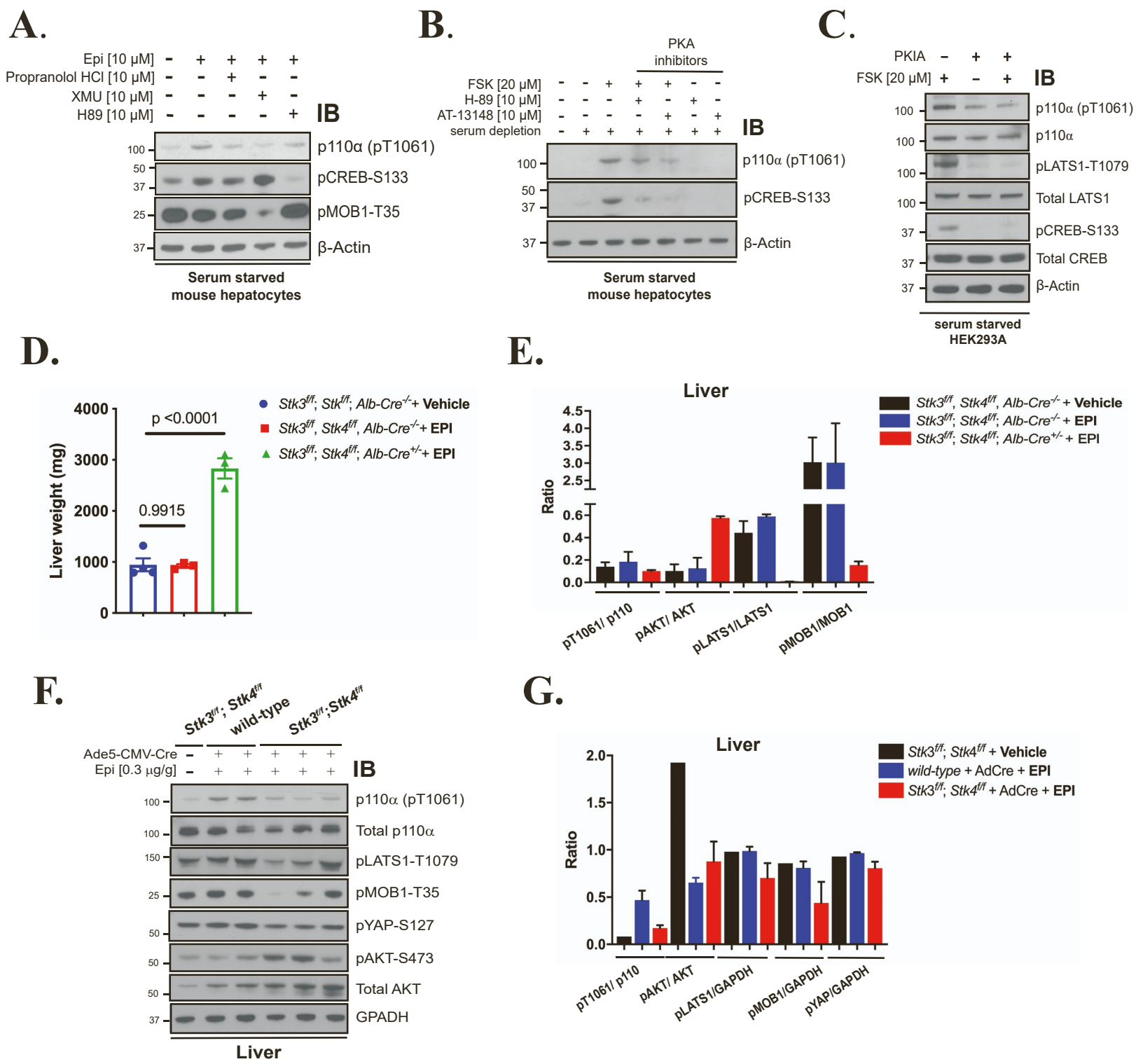

Figure S9. PKA and the Hippo kinases regulate FSK/ Epi-mediated p110α phosphorylation.

(A) Immunoblot for the indicated proteins using lysates from serum starved primary mouse hepatocytes isolated from WT mice that were treated with Epi [10 μM], or Epi with Propranolol HCl [10 μM], XMU [10 μM], or H-89 [10 μM]. (B) Immunoblot for the indicated proteins using lysates from primary mouse hepatocytes that were serum starved 12 h before stimulated with DMSO, FSK [20 μM], FSK [20 μM] with two PKA inhibitors (H-89 and AT13148) [10 μM] or inhibitors alone. (C) Immunoblot for the indicated proteins using lysates from HEK293A cells transfected with control or PKIA vector for 2 days before serum starved for 2 h, followed by stimulation with FSK [20 μM] for 15 min. (E) Quantification of the ratio of phosphorylated proteins over total proteins using band intensity from [Fig. 6E]. Data were represented as means ± SEMs. (F) Immunoblot for the indicated proteins using lysates from liver taken from $Stk3^{f/f}$; $Stk4^{f/f}$ or WT mice. Mice were injected with Ad5-CMV-Cre virus [10^9] to induce liver-specific MST1/2 gene deletion, and then two weeks later, the mice were injected with vehicle (saline) or Epi [0.3ug/g] and liver were harvested.(G) Quantification of the ratio of phosphorylated proteins over total proteins using band intensity from (F).

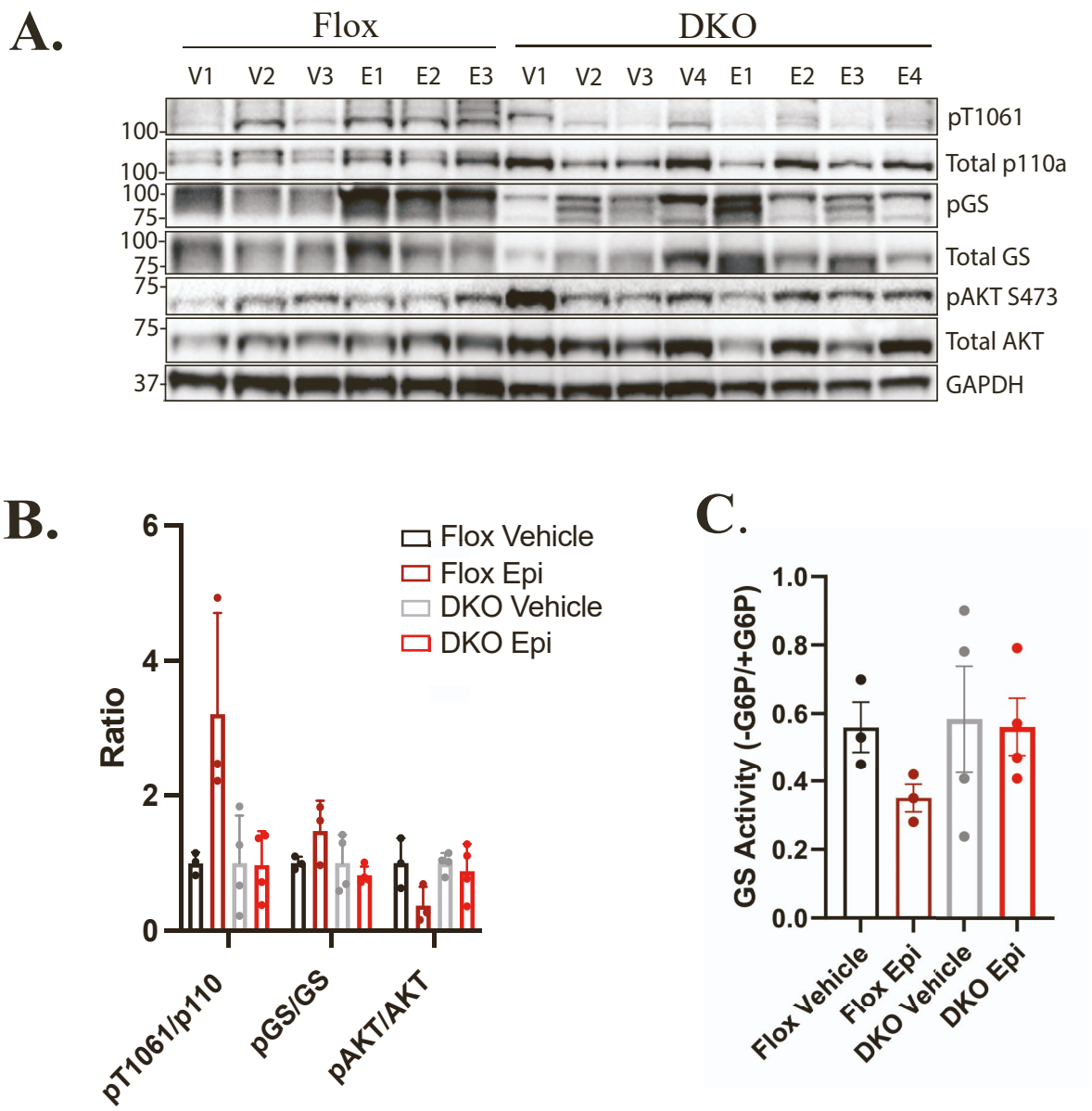

Figure S10. Epinephrine-mediated suppression of glycogen synthesis is reduced in MST1/2 DKO mice.

(A) Immunoblot for the indicated proteins using lysates from livers taken from $Stk3^{f/f}$,$Stk4^{f/f}$, Alb-$Cre^{-/-}$ (Flox) and $Stk3^{f/f}$; $Stk4^{f/f}$, Alb-$Cre^{+/-}$ (DKO) that were injected with vehicle (normal saline, V) or Epi (E) [0.3 µg/g]. N=3 (B) Quantification of the ratios of pT1061 to total p110α, pGS to total GS, pAKT to total AKT using band intensity from A. (C) Hepatic GS activity from Flox and DKO mice (N=3-4). Data is presented as Mean ± SEMs.

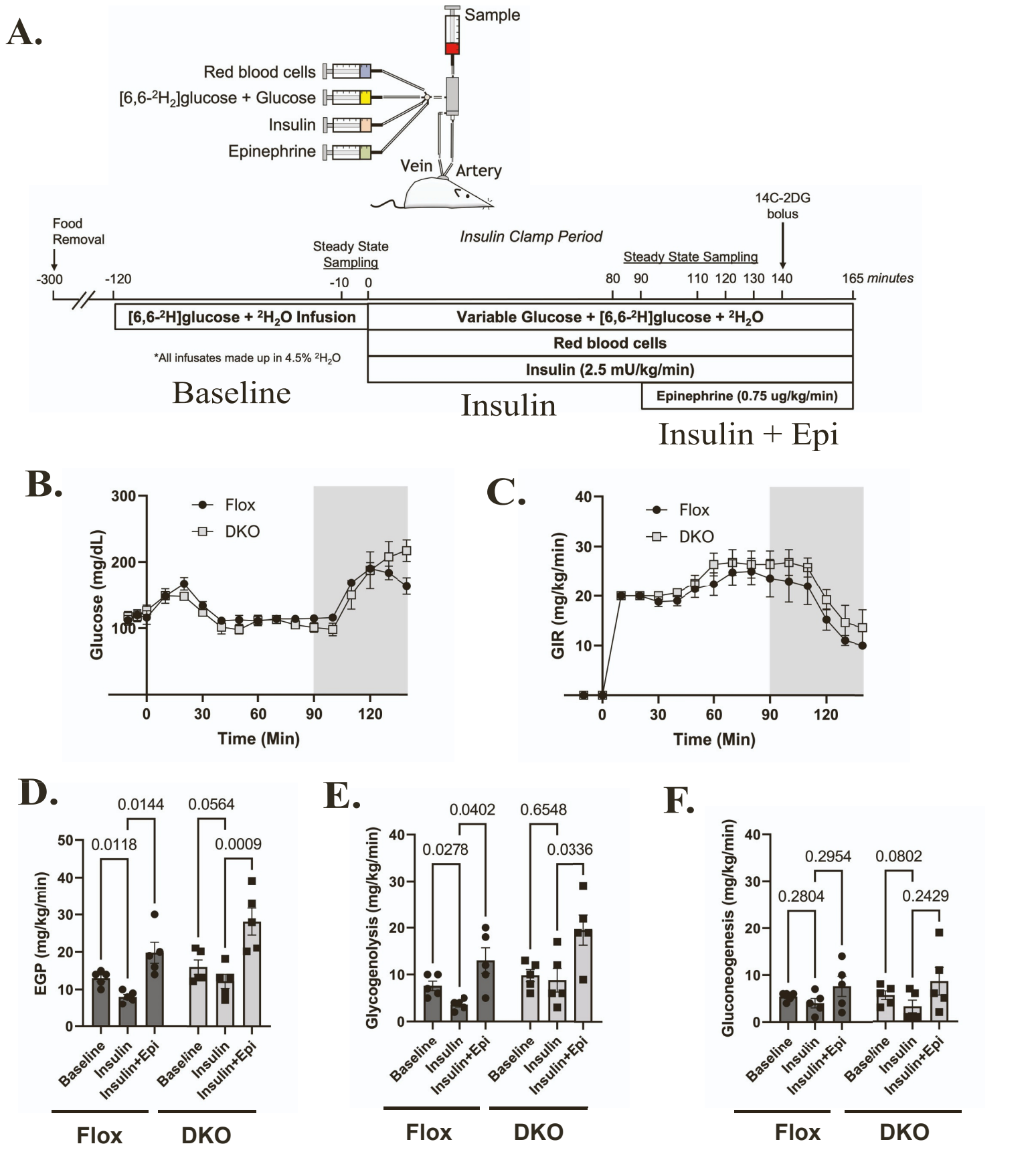

Figure S11. Epinephrine-mediated glycogenolysis is in tact in MST1/2 DKO mice under hyperinsulinemic-euglycemic conditions.

(A) Schematic describing hyperinsulinemic-euglycemic clamp (HIEC) protocol with epinephrine infusion performed on Stk3$^{f/f}$,Stk4$^{f/f}$, Alb-Cre $^{-/-}$ (Flox, N=5) and Stk3$^{f/f}$; Stk4$^{f/f}$, Alb-Cre$^{+/-}$ (DKO, N=5) mice. (B) Glucose and (C) glucose infusion rate (GIR) over time. N=5. Rates of (D) endogenous glucose production (EGP), (E) glycogenolysis, and (F) gluconeogenesis during the clamp protocol. Data presented as mean ± SEM. In D-F, comparisons made via Two-way ANOVA.